JOURNAL OF Materials CHEMISTRY

Structural characterisations of the Na_xSi_{136} and Na_8Si_{46} silicon clathrates using the Rietveld method

Edouard Reny,* Pierre Gravereau, Christian Cros and Michel Pouchard†

Institut de Chimie de la Matière Condensée de Bordeaux, UPR CNRS 9048, 87, Avenue du Docteur Albert Schweitzer, 33608 Pessac Cedex, France. E-mail: Reny@chimsol.icmcb.u-bordeaux.fr

Received 16th June 1998, Accepted 16th September 1998

The crystal structure of the non-stoichiometric Na_xSi_{136} silicon clathrate has been refined using the Rietveld method, in order to determine accurately the distribution of the sodium atoms within the two available sites. In agreement with the previous data, it was found that for $x \leqslant 8$, the alkali atoms occupy exclusively, and not only preferentially the eight larger Si_{28} sites. For $8 < x < 24$, the filling of the sixteen smaller Si_{20} cages occurs gradually with increasing x, and a slight increase of the unit cell parameter is then observed. The crystal structure of the stoichiometric Na_8Si_{46} clathrate, which is present as impurity in the studied samples, has also been refined.

Introduction

Thermal decomposition of the Zintl phase MSi (M = Na, K, Rb, Cs) under vacuum or inert atmosphere leads to the formation of clathrate type alkali metal silicides.[1–6] Depending on the alkali metal and the experimental conditions, two types of structures are formed, corresponding to the formula M_xSi_{46} ($x \approx 8$ for M = Na and K, $x \approx 6$ for M = Rb) and M_xSi_{136} (M = Na, Cs). The two structures were found to be respectively isostructural to the clathrate hydrates of type I [or gas hydrate, such as $(Cl_2)_8(H_2O)_{46}$] and type II [or liquid hydrate, such as $(CHCl_3)_8(H_2O)_{136}$ or $(H_2S)_{16}(CCl_4)_8(H_2O)_{136}$].[2,3,7] In both structures, the silicon host lattice is formed by a combination of two types of polyhedra of fullerene type, *i.e.* having only pentagonal and hexagonal faces. The basic polyhedron, which is common to the two structures, is the pentagonal dodecahedra (12 pentagonal faces), Si_{20}; it is the smallest possible fullerene type cage.

The silicon host lattice of the M_xSi_{46} structure (Fig. 1) is composed of two pentagonal dodecahedra, Si_{20} and six tetrakaïdecahedra (12 pentagonal and 2 hexagonal faces), Si_{24}. The corresponding unit cell is cubic ($a \approx 10.19$ Å) with the space group $Pm\bar{3}n$. This silicon lattice offers two sites with a $\bar{3}m$ symmetry and six sites with a $4m2$ symmetry located respectively at the (0 0 0) and (1/4 1/2 0) positions. When the trapped alkali metal is sodium or potassium, the silicon cages seem to be fully occupied leading to the stoichiometric compound M_8Si_{46}.

The silicon host lattice of the M_xSi_{136} structure (Fig. 2) is composed of 16 pentagonal dodecahedra and 8 hexakaïdecahedra (12 pentagonal and 4 hexagonal faces), Si_{28}. The unit cell is also cubic ($a \approx 14.62$ Å) with the space group $Fd\bar{3}m$. The silicon lattice offers 16 sites with a $\bar{3}m$ symmetry and 8 sites with a $4\bar{3}m$ symmetry located respectively at the (0 0 0) and (3/8 3/8 3/8) positions, consequently, the maximum authorised value for x is 24. Unlike the Na_8Si_{46} compound, M_xSi_{136} is a non-stoichiometric phase, all the cages are not necessarily occupied. Na_xSi_{136} can be obtained within a very large range of compositions depending on the experimental conditions: $1 < x < 23$.

The presence of alkali metals trapped in open host lattices made of tetrahedrally bonded covalent silicon atoms induces interesting physical properties for these compounds.[3,8,9] Following the discovery of the fullerene forms of carbon and the superconducting behaviour of the intercalation compounds M_3C_{60} or MM'_2C_{60} (M, M′ = Na, K, Rb, Cs), the silicon clathrates have been intensively reinvestigated on the theoretical and experimental viewpoints.[10–22]

† Member of the Institut Universitaire de France.

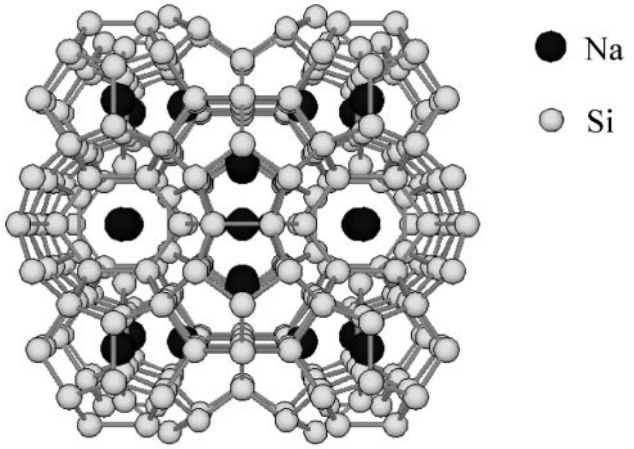

Fig. 1 Representation of the M_8Si_{46} structure.

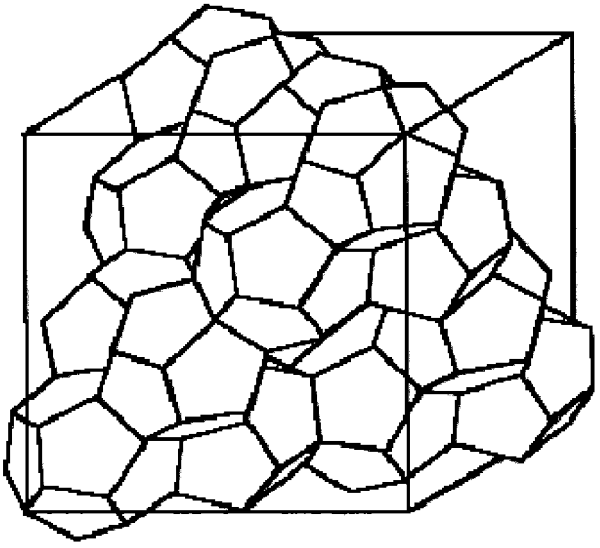

Fig. 2 Representation of the M_xSi_{136} structure.

One of the major new results was the observation of superconductivity ($T_c \approx 4$K) in the two clathrates $Na_2Ba_6Si_{46}$ and $K_2Ba_6Si_{46}$, where the six larger Si_{24} cages are occupied by barium instead of sodium and potassium respectively.[14,15,18] Other results concerning the non-stoichiometric Na_xSi_{136} phase have been obtained. For instance, a noticeable variation of the electric properties has been measured depending on the composition, from semiconductor, Na_xSi_{136} becomes progressively metallic when x increases.[7–9,19] Moreover theoretical calculation on pure Si_{136} (no alkali atoms trapped in the silicon cages) shows that the band gap opens by 0.7 eV comparatively to diamond silicon.[10–13,20] The 1.9 eV broad bandgap of this compound is very close to that of porous silicon. This could be of great interest in new electronic applications. More recently, a ^{23}Na NMR study performed on various Na_xSi_{136} samples revealed interesting information about the ionisation degree of the Na atoms encapsulated in the silicon cages. According to this technique, the electronic state of the trapped atoms is intermediate between metallic and atomic.[21–23]

The crystal structures of Na_xSi_{46} and Na_xSi_{136} have been already investigated. In the first refinement of the structure of Na_xSi_{136} with $x=9.5$, a preferential but not exclusive occupancy of the eight large Si_{28} cages was observed, the occupancy rates being respectively 0.79 and 0.21 for the large Si_{28} and the small Si_{20} sites.[2] Another calculation performed by Cros on two compositions $x=3$ and $x=10$ led to more equilibrated occupancy rates.[7] In a more recent investigation by Sim of a series of ten compositions, it was observed that the sodium atoms occupy almost exclusively the large Si_{28} cages for $x \leqslant 8$, and for $8 \leqslant x \leqslant 24$, the smaller Si_{20} sites are progressively occupied with increasing x.[9] All the above reported structural studies by XRD were performed without the use of the most advanced refinement methods, which enable to get more accurate data than previously. Furthermore, the preferential site occupancy of the large Si_{28} cages for $x \leqslant 8$ was called into question in recent work.[22]

These two reasons led us to undertake a careful investigation of the crystal structure of a series of samples of Na_xSi_{136}, with well characterised x values, by the Rietveld method. As far as the Na_8Si_{46} clathrate was present as an impurity in our samples, this latter compound was also investigated. The results of this study are reported in the present paper.

Experimental

Preparation

The clathrates Na_xSi_{136} with $x<14$ are synthesised by thermal decomposition of NaSi under vacuum (10^{-4} Pa) at temperatures between 340 and 440 °C. Those with larger values of x can be prepared in a closed steel reactor, according to the reaction: $Na_xSi_{136}+Na$ (vapour)$\rightarrow Na_{x'}Si_{136}$ ($x'>x$), in the temperature range 370–400 °C. Six samples of Na_xSi_{136} were prepared, the concentration in sodium depending on the pyrolysis temperature. Samples have been numbered with increasing values of x (Table 4). The concentration in sodium of sample VI has been raised to $x=20.5$ by a thermal treatment under sodium vapour. All these samples contained some amounts of the second phase, Na_8Si_{46}.

The clathrate Na_8Si_{46} has been synthesised by thermal decomposition of NaSi under argon at 410 °C. It contained small amounts of the other phase, Na_xSi_{136} with $x>20$.

X-Ray diffraction patterns acquisition

The powder diffraction patterns were collected on a X'PERT MPD (θ-θ) Philips diffractometer (Cu-Kα, graphite monochromator, 40 kV, 40 mA, receiving slit: 50 μm, angular range: 10–120° (2θ), counting time: 30 s by steps of 0.02° (2θ), sample rotation, room temperature).

General information on the Rietveld refinements

Rietveld refinements have been performed on each XRD pattern using the FULLPROF program.[24] For every diffractogram, the following parameters have been refined: the zero point, one asymmetry parameter, the six background polynomial parameters, the three full width at half maximum (H_k) parameters of the Cagliotti law: $H_k^2 = U\tan^2\theta + V\tan\theta + W$, the η parameter of the pseudo–Voigt fonction, *i.e.* representing the combination of a Lorentzian and a Gaussian type of peak [$PV=\eta L+(1\text{-}\eta)G$], the scale factor, the atomic positions, the isotropic thermal agitation factors of the silicon and sodium atoms.

For every diffractogram, the observed peaks are very close to the Lorentzian type ($0.8<\eta<0.9$). Consequently, the contribution of a peak at $2\theta_p$ is taken into account between $2\theta_p - 20H_k$ and $2\theta_p + 20H_k$.

Due to correlation between the rate of occupancy and the thermal agitation parameters of the sodium atoms, it was necessary to fix the sodium concentration x to the values found in analysis. The reliability factors used are defined in Table 2. Standard deviation was calculated taking into account the Berar factor to correct local correlations.[25]

Determination of the sodium ratio in Na_xSi_{136}

The global sodium content for each sample has been determined by X-ray microprobe using an E.P.M.A. Cameca SX-100 apparatus. The values obtained have been confirmed by flame emission technique with a Perkin Elmer 306 double beam spectrometer.

To obtain a reliable value of x in Na_xSi_{136}, it is necessary to determine the relative amount of the Na_8Si_{46} impurity phase. The mass ratio w_j of each phase has been approached by quantitative phase analysis using the Rietveld method:

$$w_j(\%) = 100 \times \frac{S_j Z_j M_j V_j}{\sum_i^n (S_i Z_i M_i V_i)}$$

where S_j is the scale factor for phase j, M_j the mass of the formula unit, Z_j the number of formula units per unit cell and V_j the volume of the unit cell. This allowed a correction on the experimental value of x which was fixed in the final Rietveld refinements (Table 4). The similar isotropic thermal parameters found for the Na atoms in the different Rietveld refinements constitute an indirect confirmation of the x fixed values.

Structural characterisation of the Na_8Si_{46} compound

The XRD pattern of Na_8Si_{46} (Fig. 3) revealed the existence of a minor impurity phase Na_xSi_{136} (*ca.* 7.7% in weight). A ^{23}Na NMR spectrum obtained on this sample showed that the impurity compound was very rich in sodium: thus x has been considered equal to 24.[21] Due to a very weak quantity of amorphous phase in the range 10–40° range (2θ), a fifth order polynomial could not fit well the background of all the XRD pattern. Consequently a background file was generated in the following way: in the 10–40° (2θ) angular range, background points were manually determined from the XRD pattern; for $2\theta>40°$, the corresponding background points file was generated from the fifth order polynomial refined for this range, with the 'pattern-matching' option of the FULLPROF program.

In a 10–120° (2θ) angular range, 161 reflections were obtained for the major compound Na_8Si_{46} and 141 for the minor $Na_{24}Si_{136}$ phase. The powder diffraction data extracted for Na_8Si_{46} are listed in Table 1. The final results (Table 2) obtained from the refinement of 29 parameters led to atomic positions of the silicon atoms with similar thermal parameters. These values are very close to those obtained previously by

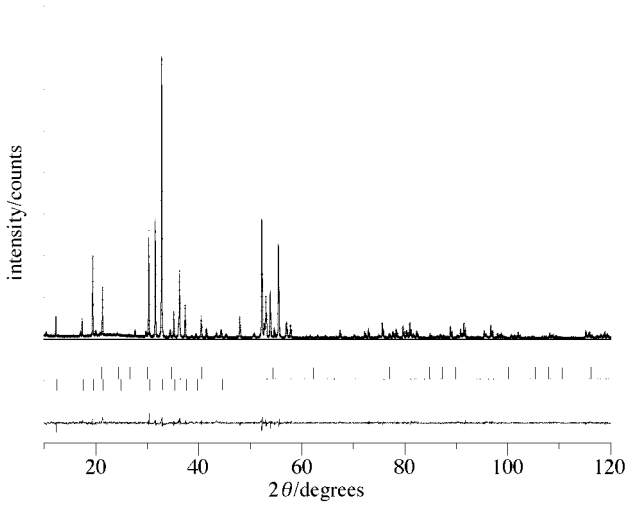

Fig. 3 Final Rietveld plot to the X-ray diffraction for Na_8Si_{46}. The crosses represent the experimental data points and the upper continuous line the calculated spectra. The upper tick marks indicate the calculated reflection positions for the minor impurity phase Na_xSi_{136} and the lower tick marks the calculated reflection position of Na_8Si_{46}. The lower continuous line represents the difference.

Table 1 Powder diffraction data of Na_8Si_{46} (Cu-Kα; $\lambda = 1.540\,60$ Å)

h	k	l	d_{calc}	I_{calc}	h	k	l	d_{calc}	I_{calc}
1	1	0	7.211	30.9	5	1	0	2.000	10.6
2	0	0	5.099	27.2	4	3	1	2.000	<1
2	1	0	4.561	152.3	5	2	0	1.894	14.8
2	1	1	4.163	85.7	4	3	2	1.894	47.2
2	2	0	3.606	<1	5	2	1	1.862	<1
3	1	0	3.225	11.0	4	4	0	1.803	4.2
2	2	2	2.944	231.9	5	3	0	1.749	250.7
3	2	0	2.829	239.3	4	3	3	1.749	110.0
3	2	1	2.726	692.3	5	3	1	1.724	124.1
4	0	0	2.550	64.1	6	0	0	1.700	89.7
4	1	0	2.473	157.5	4	4	2	1.700	45.5
3	3	0	2.404	79.8	6	1	0	1.677	28.0
4	1	1	2.404	1.1	6	1	1	1.654	34.0
4	2	0	2.280	8.9	5	3	2	1.654	255.1
4	2	1	2.225	52.4	6	2	0	1.613	42.8
3	3	2	2.174	23.4	5	4	0	1.593	28.9
4	2	2	2.082	7.8	6	2	1	1.593	12.1
4	3	0	2.040	21.5	5	4	1	1.574	1.2

Table 2 Atomic parameters and R factors[a] for Na_8Si_{46} in space group $Pm\bar{3}n$

Atom	Site	x	y	z	B_{iso}/Å^2
Si(1)	6c	0.25	0	0.5	1.13(11)
Si(2)	16i	0.1847(2)	0.1847(2)	0.1847(2)	1.08(6)
Si(3)	24k	0	0.3088(2)	0.1173(2)	1.03(5)
Na(1)	2a	0	0	0	2.5(3)
Na(2)	6d	0.25	0.5	0	3.6(2)

Cell parameter/Å	10.1983(2)		
Volume/Å^3	1060.67(5)		
D_x/g cm^{-3}	2.311		
η	0.43(1)		
Profile parameters	$U_1 = 0.000(1)$	$V_1 = 0.013(2)$	$W_1 = 0.040(5)$
Rietveld reliability factors:	$cR_p = 0.145$	$cR_{wp} = 0.177$	$\chi^2 = 1.56$
	$R_p = 0.0889$	$R_{wp} = 0.127$	
	$R_I = 0.0426$	$R_f = 0.0438$	

The R factors are defined as $cR_p = \sum_i |y_{io} - y_{ic}| / \sum_i |y_{io} - y_{ib}|$, $cR_{wp} = (\sum_i w_i (y_{io} - y_{ic})^2 / \sum_i w_i (y_{io} - y_{ib})^2)^{1/2}$, $\chi^2 = \sum_i w_i (y_{io} - y_{ic})^2 / (N - P + C)$, $R_p = \sum_i |y_{io} - y_{ic}| / \sum_i y_{io}$, $R_{wp} = (\sum_i w_i (y_{io} - y_{ic})^2 / \sum_i w_i y_{io}^2)^{1/2}$, $R_I = \sum_k |I_{ko} - I_{kc}| / \sum_k I_{ko}$, $R_F = \sum_k |F_{ko} - F_{kc}| / \sum_k F_{ko}$.

some of us.[7] No preferred orientation correction was applied. One asymmetry correction parameter has been refined for values of $2\theta < 40°$. A list of the interatomic distances and angles is presented in Table 3 and visualised in Fig. 4. The average interatomic Si–Si distance is 2.369 Å and is close to the value in diamond-type silicon (2.352 Å). The observed Si–Si–Si bond angles range from *ca.* 105 to *ca.* 125° and the average value is close to 109.54°, which is characteristic of an sp^3 hybridisation. The calculated 'free radius' of the Si_{20} cages, based on the eight shortest Na(1)–Si(2) distances ($r_1^{46} = d_{Na(1)Si(2)} - r_{Si}$), is 2.08 Å. The 'free radius' of the Si_{24} larger cages (r_2^{46}) is 2.241 Å. The volume per formula unit of the clathrate type silicon host lattice is $V/Z = 23.058$ Å^3, *cf.* 20.023 Å^3 in diamond-type silicon. Consequently, the clathrate type silicon network is 15.2% more open.

Structural characterisation of the Na_xSi_{136} compound

Fourier difference functions have been calculated using the SHELXL 93 program.[26] The difference between Fourier transformation of the structural factors observed for Na_xSi_{136} ('F_{obs}') obtained *via* FULLPROF and the calculated structural factors of the empty silicon lattice Si_{136}, (F_{calc}), provides us with a map of electronic densities attributed to the sodium atoms. This study, performed with the diffraction pattern of sample II ($x = 3$) revealed the two important following points: (i) there is no sodium in the pentagonal dodecahedric sites for $x \leqslant 8$ and (ii) the residual electronic density appears clearly in the centre of the Si_{28} cage (3/8 3/8 3/8). This rules out the hypothesis of a decentering of the sodium atoms in the silicon cages, that could have been envisaged considering the relatively high value of the isotropic atomic displacement parameter ($B \approx 8$ Å^2).

In the case of sample V, where the value of x in Na_xSi_{136} is higher than the number of available Si_{28} sites ($x = 13.6$), this study shows a full occupation of the Si_{28} cages, the remaining sodium atoms being perfectly centred in the pentagonal dodecahedric cages (16c sites).

It is now possible to fix the atomic positions of the sodium atoms and, knowing the global composition of Na_xSi_{136}, to define the rate of occupancy of the two types of sodium sites in all samples. In sample VI, a weak amorphous contribution, probably linked to a high concentration in Na_8Si_{46} ($\approx 13\%$) compound, led to a background determination in two steps, as seen previously for Na_8Si_{46} and allowed us to release atomic

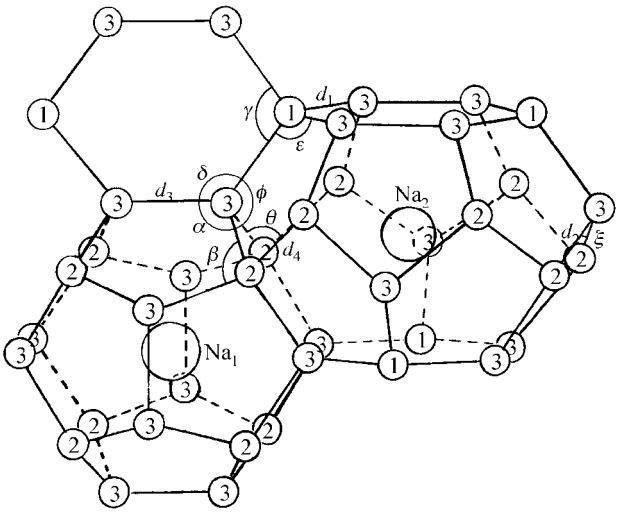

Fig. 4 Representation of two connected cages in the Na_8Si_{46} structure. The eight non-equivalent bonding angles and the four Si–Si distances are indicated.

Table 3 List of refined interatomic distances (Å) and angles (°) for Na_8Si_{46}

Si–Si	d_1=Si(1)–Si(3)	2.373(2)	Na–Si	Na(1)–Si(2)	3.263(2)
	d_2=Si(2)–Si(3)	2.371(2)		Na(1)–Si(3)	3.369(2)
	d_3=Si(3)–Si(3)	2.393(3)		Na(2)–Si(1)	3.606(1)
	d_4=Si(2)–Si(2)	2.306(2)		Na(2)–Si(2)	3.786(2)
				Na(2)–Si(3)	3.425(2), 3.948(2)
angles on Si(1)	γ=Si(3)–Si(1)–Si(3)	110.5(1)	angles on Si(3)	φ=Si(1)–Si(3)–Si(2)	105.9(1)
	ε=Si(3)–Si(1)–Si(3)	109.0		δ=Si(1)–Si(3)–Si(3)	124.8(1)
angles on Si(2)	θ=Si(2)–Si(2)–Si(3)	108.5(1)		ξ=Si(2)–Si(3)–Si(2)	105.2(1)
	β=Si(3)–Si(2)–Si(3)	110.4		α=Si(3)–Si(3)–Si(2)	106.8(1)

positions and average isotropic thermal factors for this compound.

Results of the Rietveld refinements for all samples are presented in Table 5 and 6. Fig. 5(a) and (b) present two examples of the refined XRD patterns (sample II and VI). Interatomic distances and bond angles for these two samples are presented in Table 7. They are visualised on Fig. 6.

In the highly non-stoichiometric Na_3Si_{136} compound, the average Si–Si distance is 2.360 Å (2.352 Å in diamond-type silicon). The Si–Si–Si bonding angles range from *ca.* 105.7 to *ca.* 120°. The calculated 'free radius' of the Si_{28} cage (r_2^{136}= $d_{Na(1)Si(3)}-r_{Si}$), based on the shortest Na(1)–Si(3) distance, is 2.722 Å. The 'free radius' of the empty Si_{20} cages is r_1^{136}= 1.990 Å ($r_1^{136}=d_{Na(2)Si(1)}-r_{Si}$). In the almost stoichiometric $Na_{20.5}Si_{136}$ clathrate, the average Si–Si distance is 2.371 Å and the values of r_2^{136} and r_1^{136} are 2.724 and 1.998 Å respectively. All these data are consistent with the results of previous work.[2,7,9] They confirm that the free radius of the Si_{20} cages is slightly smaller in the Si_{136} clathrate than in the Si_{46} one ($r_1^{136}\approx 2.00$ Å instead of $r_1^{46}\approx 2.08$ Å).

No noticeable structural evolution, *i.e.* variation in the lattice parameter and the atomic positions, occurs in sample I, II and III. Sample IV–VI see their lattice parameters increasing slightly but significantly with the sodium concentration, *i.e.* when the Si_{20} cages start to fill up (Fig. 7) and is another point that is in favour of the preferential occupancy of the Si_{28} sites. ^{23}Na NMR spectra acquired on various Na_xSi_{136} samples showed that the trapped Na atoms tend to conserve their 3s electron density and consequently can be described as in a state between metallic and neutral, *i.e.* their radius is situated between 1.54 and 2.30 Å.[27] As the free radius of the Si_{20} cages (r_1^{136}) is *ca.* 1.99 Å, sodium atoms would be less likely to intercalate in these cages than in the wider Si_{28} cages ($r_2^{136}\approx 2.72$ Å). When the pentagonal dodecahedra start

Table 4 List of the Na_xSi_{136} samples studied

Sample	I	II	III	IV	V	VI
Pyrolysis temp. °C	440	400	370	340	340	Na_{vap}[a]
x in Na_xSi_{136}	1.0±0.5	3.0±0.8	3.8±0.4	10.5±0.5	13.6±1.2	20.5±1.5
Si_{20} occupancy	0.0	0.0	0.0	0.15	0.35	0.78
Si_{28} occupancy	0.125	0.375	0.475	1.0	1.0	1.0
Weight ratio in Na_8Si_{46} (%)	1.8	4.7	9.5	2.9	6.9	12.8

[a]Sample VI has been obtained by submitting Na_6Si_{136} (previously synthesised) under a sodium vapor atmosphere for 30 h at 320 °C.

Table 5 Refined atomic positions of Na_xSi_{136} in samples I–VI

	Atom [site]	x	y	z	B_{iso}/Å^2
Sample I	Si(1) [2a]	0.125	0.125	0.125	0.49(18)
(Na_1Si_{136})	Si(2) [32c]	0.2173(2)	0.2173(2)	0.2173(2)	0.45(10)
	Si(3) [96g]	0.1831(1)	0.1831(1)	0.3712(2)	0.50(6)
	Na(1) [8b]	0.375	0.375	0.375	6.9(2.7)
Sample II	Si(1) [2a]	0.125	0.125	0.125	0.29(16)
(Na_3Si_{136})	Si(2) [32c]	0.2174(2)	0.2174(2)	0.2174(2)	0.26(9)
	Si(3) [96g]	0.1830(1)	0.1830(1)	0.3714(1)	0.35(5)
	Na(1) [8b]	0.375	0.375	0.375	5.6(1.1)
Sample III	Si(1) [2a]	0.125	0.125	0.125	0.27(12)
($Na_{3.8}Si_{136}$)	Si(2) [32c]	0.2174(1)	0.2174(1)	0.2174(1)	0.28(7)
	Si(3) [96g]	0.1830(1)	0.1830(1)	0.3712(1)	0.49(4)
	Na(1) [8b]	0.375	0.375	0.375	8.2(9)
Sample IV	Si(1) [2a]	0.125	0.125	0.125	0.49(16)
($Na_{10.4}Si_{136}$)	Si(2) [32c]	0.2175(1)	0.2175(1)	0.2175(1)	0.53(10)
	Si(3) [96g]	0.1831(1)	0.1831(1)	0.3712(2)	0.59(5)
	Na(1) [8b]	0.375	0.375	0.375	2.2(1.3)
	Na(2) [16c]	0	0	0	9.6(5)
Sample V	Si(1) [2a]	0.125	0.125	0.125	0.41(12)
($Na_{13.6}Si_{136}$)	Si(2) [32c]	0.2178(1)	0.2178(1)	0.2178(1)	0.38(7)
	Si(3) [96g]	0.1831(1)	0.1831(1)	0.3715(1)	0.39(4)
	Na(1) [8b]	0.375	0.375	0.375	1.9(4)
	Na(2) [16c]	0	0	0	8.9(4)
Sample VI	Si(1) [2a]	0.125	0.125	0.125	0.35(18)
($Na_{20.5}Si_{136}$)	Si(2) [32c]	0.2186(2)	0.2186(2)	0.2186(2)	0.43(10)
	Si(3) [96g]	0.1832(1)	0.1832(1)	0.1722(2)	0.45(5)
	Na(1) [8b]	0.375	0.375	0.375	0.7(2)
	Na(2) [16c]	0	0	0	7.8(6)

Table 6 Results from the refinements of Na_xSi_{136} in samples I–VI

	Sample I	Sample II	Sample III	Sample IV	Sample V	Sample VI
Formula	Na_1Si_{136}	Na_3Si_{136}	$Na_{3.8}Si_{136}$	$Na_{10.4}Si_{136}$	$Na_{13.6}Si_{136}$	$Na_{20.5}Si_{136}$
a/Å	14.6428(8)	14.6410(6)	14.6426(5)	14.6449(8)	14.6607(6)	14.7030(5)
Cell volume/Å^3	3139.5(2)	3138.4(1)	3139.4(1)	3140.9(2)	3151.1(1)	3178.5(1)
D_x/g cm^{-3}	2.032	2.057	2.066	2.146	2.178	2.242
η	0.81(3)	0.89(2)	0.94(2)	0.87(2)	0.76(2)	0.84(3)
Caglioti coeff.						
U	0.13(2)	0.106(10)	0.119(10)	0.136(16)	0.20(2)	0.19(1)
V	−0.033(12)	−0.035(7)	−0.033(7)	−0.031(12)	−0.035(11)	−0.022(8)
W	0.024(2)	0.016(1)	0.020(1)	0.021(2)	0.022(2)	0.015(2)
Rietveld factors						
cR_p	0.115	0.110	0.108	0.117	0.099	0.107
cR_{wp}	0.148	0.146	0.138	0.148	0.127	0.127
χ^2	2.43	2.54	1.85	1.97	1.85	3.31
R_p	0.0883	0.0872	0.0820	0.0832	0.0764	0.0712
R_{wp}	0.120	0.123	0.111	0.114	0.104	0.0941
R_I	0.0488	0.0484	0.0385	0.0398	0.0328	0.0562
R_F	0.0296	0.0287	0.0241	0.0250	0.0220	0.0355

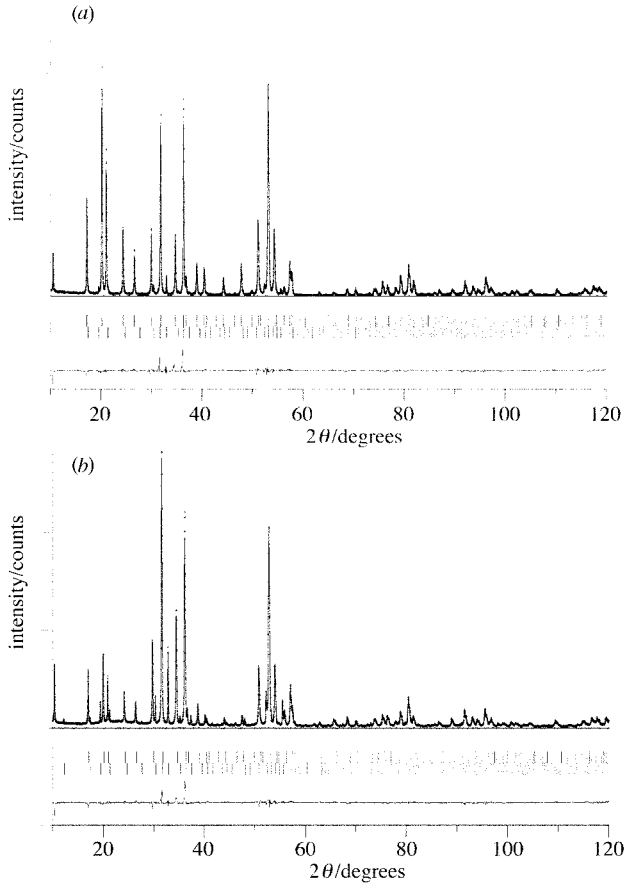

Fig. 5 Final Rietveld plot of the X-ray diffraction data for (a) sample II and (b) sample VI. The crosses represent the experimental data points and the upper continuous line the calculated spectra. The upper tick marks indicate the calculated reflection positions for the major phase Na_xSi_{136} and the lower ticks marks the calculated reflection position of the impurity phase Na_8Si_{46}. The lower continuous line represents the difference.

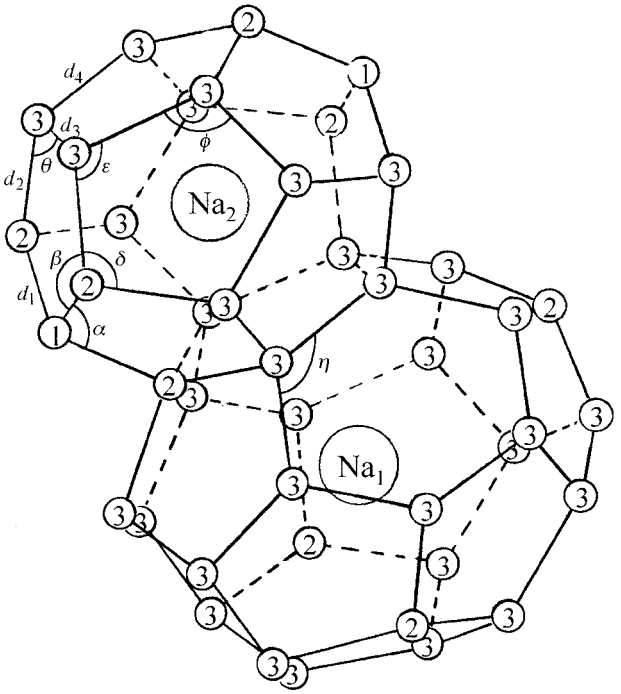

Fig. 6 Representation of two connected cages in the Na_xSi_{136} structure. The seven non-equivalent bonding angles and the four Si–Si distances are indicated.

to fill up, strain caused by the guest atoms seems to have a steric influence on the host atomic positions and extends the lattice parameter.

Conclusion

The present study confirms the previously reported data on the crystal structure of the two clathrates Na_xSi_{46} and Na_xSi_{136}. In Na_xSi_{46}, both the two Si_{20} and six Si_{24} sites are fully occupied by sodium atoms, involving the value $x=8$ and the formulation Na_8Si_{46}. In the case of Na_xSi_{136}, our results show unambiguously that the sodium atoms are exclusively, and not only preferentially, located in the eight large Si_{28} sites for $x \leqslant 8$, and that for $8 < x \leqslant 24$, the smaller Si_{20} sites are progressively occupied with increasing x. These results are consistent with those of our study by ^{23}Na NMR spectroscopy of the two clathrates.[21] In Na_8Si_{46}, two sharp lines with a shift of 1766 and 2019 ppm are observed, which have been identified to correspond to sodium atoms in the Si_{20} and Si_{24} cages, respectively. In the case of Na_xSi_{136}, a broad line, centred at *ca.* 1800 ppm is observed in the composition range $x \leqslant 8$. Then, with increasing x, this broad line exhibits two components which are finally resolved into two sharp lines located at 1608 and 1812 ppm for $x > 20$. These two sharp lines, which have been related to the appearance of metallic-like conductivity, have been attributed to sodium atoms in the eight Si_{28} and sixteen Si_{20} sites, respectively.

Similar results, as to the position of the lines for the two clathrates have been recently reported by other authors.[23]

Table 7 List of refined interatomic distances (Å) and angles (°) for Na_xSi_{136} (sample II and VI)

Sample II					
Si–Si	d_1 = Si(1)–Si(2)	2.343(2)	Na–Si	Na(1)–Si(2)	3.997(2)
	d_2 = Si(2)–Si(3)	2.365(3)		Na(1)–Si(3)	3.975(2)
	d_3 = Si(3)–Si(3)	2.339(3)		Na(1)–Si(3)	3.902(3)
	d_4 = Si(3)–Si(3)	2.403(2)			
angles on Si(1)	α = Si(2)–Si(1)–Si(2)	109.5(1)	angles on Si(3)	ε = Si(2)–Si(3)–Si(3)	105.7(2)
				θ = Si(2)–Si(3)–Si(3)	107.5(1)
angles on Si(2)	β = Si(1)–Si(2)–Si(3)	107.8(1)		η = Si(3)–Si(3)–Si(3)	119.9(1)
	δ = Si(3)–Si(2)–Si(3)	111.1(2)		ϕ = Si(3)–Si(3)–Si(3)	108.7(1)
Sample VI					
Si–Si	d_1 = Si(1)–Si(2)	2.383(3)	Na–Si	Na(1)–Si(2)	3.983(2)
	d_2 = Si(2)–Si(3)	2.376(3)		Na(1)–Si(3)	3.989(2)
	d_3 = Si(3)–Si(3)	2.338(3)		Na(1)–Si(3)	3.909(3)
	d_4 = Si(3)–Si(3)	2.420(3)		Na(2)–Si(1)	3.183(1)
				Na(2)–Si(2)	3.280(3)
				Na(2)–Si(3)	3.384(3)
angles on Si(1)	α = Si(2)–Si(1)–Si(2)	109.5(2)	angles on Si(3)	ε = Si(2)–Si(3)–Si(3)	105.3(2)
				θ = Si(2)–Si(3)–Si(3)	108.1(2)
angles on Si(2)	β = Si(1)–Si(2)–Si(3)	107.2		η = Si(3)–Si(3)–Si(3)	119.8(2)
	δ = Si(3)–Si(2)–Si(3)	111.6(2)		ϕ = Si(3)–Si(3)–Si(3)	108.8(2)

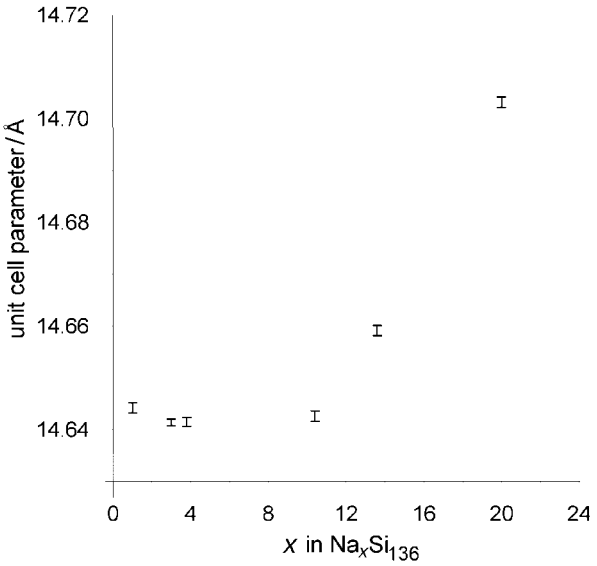

Fig. 7 Plot of the lattice parameter of Na_xSi_{136} *vs.* x.

However, these authors observe the two sharp lines of Na_xSi_{136} for a value of x as low as 9 (determined from a density measurement), a result which implies that the two available sites are almost equally occupied by sodium atoms. The departure of these data from our own data seems to be due to a difference in the value of x, since we only observe the two sharp lines for the highest values of x, *i.e.* $x > 20$.

References

1 C. Cros, M. Pouchard and P. Hagenmuller, *C.R. Acad. Sci.*, 1965, **260**, 4764.
2 J. S. Kasper, P. Hagenmuller, M. Pouchard and C. Cros, *Science*, 1965, **150**, 1713.
3 C. Cros, M. Pouchard and P. Hagenmuller, *J. Solid State Chem.*, 1970, **2**, 570.
4 C. Cros and J. C. Benejat, *Bull. Soc. Chim. Fr.*, 1972, **5**, 1739.
5 J. Gallmeier, H. Schäfer and A. Weiss, *Z. Naturforsch. Teil B*, 1967, **22**, 1080.
6 J. Gallmeier, H. Schäfer and A. Weiss, *Z. Naturforsch. Teil B*, 1969, **24**, 665.
7 C. Cros, PhD Thesis, 1970, Univ. Bordeaux I, no. 291.
8 N. F. Mott, *J. Solid State Chem.*, 1973, **6**, 348.
9 K. E. Sim, PhD Thesis, 1983, Imperial College of Science and Technology, London.
10 G. B. Adams, M. O'Keefe, A. A. Demkov, O. F. Sankey and Y. M. Huang, *Phys. Rev. B*, 1994, **49**, 8048.
11 A. A. Demkov, O. F. Sankey, K. E. Schmidt, G. B. Adams and M. O'Keefe, *Phys. Rev. B*, 1994, **50**, 17001.
12 S. Saito and A. Oshiyama, *Phys. Rev. B*, 1995, **51**, 2628.
13 V. I. Smelyanski and J. S. Tse, *Chem. Phys. Lett.*, 1997, **264**, 459.
14 H. Kawaji, H. Horie, S. Yamanaka and M. Ishikawa, *Phys. Rev. Lett.*, 1995, **74**, 1427.
15 S. Yamanaka, H. Horie, H. Kawaji and M. Ishikawa, *Eur. J. Solid State Inorg. Chem.*, 1995, **32**, 799.
16 P. Mélinon, P. Kéghélian, X. Blase, J. Le Brusc, A. Perez, E. Reny, C. Cros and M. Pouchard, *Phys. Rev. Lett.*, to be published.
17 Y. Guyot, B. Champagnon, E. Reny, C. Cros, M. Pouchard, P. Melinon, A. Perez and I. Gregora, *Phys. Rev. B*, 1998, **57**, 9475.
18 F. Shimizu, Y. Maniwa, K. Kume, H. Kawaji, S. Yamanaka and M. Ishikawa, *Synth. Met.*, 1997, **86**, 2141.
19 S. Roy, K. E. Sim and A. D. Caplin, *Philos. Mag. B*, 1992, **65**, 1445.
20 M. Menon, E. Richter and K. R. Subbaswamy, *Phys. Rev. B*, 1997, **56**, 1290.
21 E. Reny, M. Ménétrier, C. Cros, M. Pouchard and J. Sénégas, *C.R. Acad. Sci., Ser. IIc*, 1998, **1**, 129.
22 J. Gryko, P. F. McMillan and O. F. Sankey, *Phys. Rev. B*, 1996, **54**, 3037.
23 J. Gryko, P. F. McMillan, R. F. Marzke, A. P. Dodokin, A. A. Demkov and O. F. Sankey, *Phys. Rev. B*, 1998, **57**, 4172.
24 J. Rodriguez-Carvajal, A program for Rietveld refinement and pattern matching analysis, *Collected Abstracts of Powder Diffraction Meeting*, 1990, Toulouse, p. 127.
25 J. F. Berar and P. Lelann, *J. Appl. Crystallogr.*, 1991, **24**, 1.
26 G. M. Sheldrick, SHELXL 93, a program for the refinement of crystal structure, Univ. Göttingen, 1993.
27 J. E. Huheey, E. A. Keiter and R. L. Keiter, *Chimie Inorganique*, De Boeck, University, Bruxelles, 1996.

Paper 8/04565H